Simple Approximate Message Passing for Network Synchronization and Localization

Maria Samonaki*, † and Aggelos Bletsas*, ‡
*School of Electrical and Computer Engineering, Technical University of Crete, Chania, Greece
†Chair of Communication Networks (LKN), Technical University of Munich (TUM), Munich, Germany
‡Winlab, Department of ECE, Rutgers University, The State University of New Jersey, USA
Email: maria.samonaki@tum.de, aggelos@telecom.tuc.gr

***Abstract*—This paper revisits the problem of time synchronization and localization in wireless networks with approximate message passing. A simple yet efficient, approximate Gaussian Belief Propagation (GBP) algorithm for cooperative localization is proposed. Compared to prior art, the algorithm exploits only one-way measurements, as well as simplified equations, not offered before in the literature. The joint time offset and location estimation problem is then studied, and a non-cooperative approximate GBP algorithm is proposed, where agents communicate only with anchors, again with one-way (and not round-trip) measurements. Both proposed algorithms perform close to state-of-the-art methods while offering minimal total communication overhead, which for localization, is smaller by a factor of 100 compared to the prior art.**

***Index Terms*—Network Synchronization, Localization, Message Passing, Gaussian Belief Propagation (GBP)**

I. Introduction

In many wireless network applications, position information is vital. Thus, cooperative localization algorithms have been proposed [1]–[4] that utilize range measurements and information exchange between neighboring nodes in a peer-to-peer fashion. Ranging measurements are usually based on the pairwise calculation of the signal propagating time-of-flight, and thus, clock (time) synchronization among the network nodes is essential [5], [6].

Synchronization and localization in wireless networks have been studied both in a sequential manner - by first synchronizing the nodes to the reference time and then locating them, and jointly - by performing simultaneous clock and location estimation [7], [8]. Regarding the latter approach, particle-based implementation presented increased complexity and communication overhead. Work in [9] aimed to overcome such problems, performing cooperative synchronization and localization simultaneously by utilizing a Taylor approximation that linearized the observation function. It then applied Gaussian Belief Propagation (GBP) on the factor graph, mapped through the original network, obtaining time offset and location estimates. The joint cooperative estimation problem towards lower complexity and reduced communication overhead has also been addressed in [10], [11], [12].

In this paper, we first approach the problem sequentially and time-synchronize the nodes using the work in [5]. We then propose a quite simple yet efficient, approximate GBP-based algorithm for cooperative localization (namely CLBP), exploiting a simplified factor graph, as well as a simplified Taylor expansion compared to [9]. We then study the joint synchronization and localization problem and propose an approximate GBP for joint non-cooperative estimation (namely JNCE), where agents communicate only with anchors. In sharp contrast to prior art, this work:

1) Offers simple, easy to calculate, algebraic equations for each message, not offered before in the literature, to the best of our knowledge.
2) Utilizes only one-way measurements (instead of round-trip) and, correspondingly, simplified factor graphs in both CLBP and JNCE.
3) Minimizes total communication overhead by a factor of 100, as the exchanged messages consist of a pair of real numbers (instead of probability density functions).

II. System Model

This work assumes a wireless network with $\mathcal{M} = \{1, \ldots, M\}$ set of agent nodes to be located and time-synchronized and $\mathcal{A} = \{1, \ldots, A\}$ set of anchor nodes with known coordinates and time-synchronized at the same reference time. The local clock of each node i follows:

$$c_i(t) = \phi_i \, t + \theta_i, \tag{1}$$

where t is the accurate reference time, θ_i, ϕ_i is the time and frequency offset of node i, respectively. If $i \in \mathcal{A}$, then $\theta_i = 0$ and $\phi_i = 1$. If node i and node j are within a reliable communication range, these nodes are considered neighbors. The set of all available communication links is denoted as Ξ and the set of neighbors of node i as $N(i)$; $N(i)/j$ denotes the elements of the set, excluding j.

At time t_1, node i transmits its current timing information to node j (Fig. 1). After delay Δ_{ij}, node j receives the timing information from node i at time t_2. Node j sends back a signal at t_3, and node i captures the backward signal after delay Δ_{ji}, at t_4. Based on the location of each node $i \in \mathcal{M} \cup \mathcal{A}$, $\mathbf{x}_i = [x_i \;\; y_i]^T$, the delay Δ_{ij} is the signal propagating time $\frac{d_{ij}}{c}$, with $d_{ij} = ||\mathbf{x}_j - \mathbf{x}_i||$ the Euclidean distance and c the speed of light; thus, $\Delta_{ij} = \Delta_{ji}$. The measured timestamp at the receiver j is modeled as follows:

$$c_j(t_2) = \phi_j \left(\frac{c_i(t_1) - \theta_i}{\phi_i} + \frac{d_{ij}}{c} + u_{ij} \right) + \theta_j, \tag{2}$$

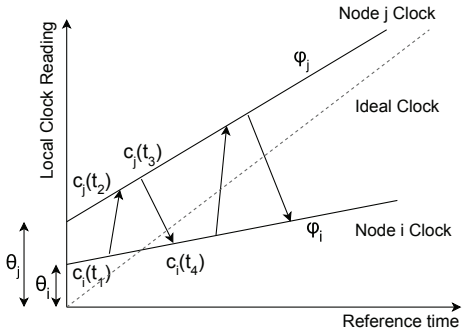

Fig. 1: Two-way synchronization messages between node i and node j.

where u_{ij} is assumed to be Gaussian distributed noise.

If the frequency skew is 0 and thus, $\phi_i = 1\ \forall i$, the observed signal propagation time can be obtained from timestamps $c(t)$ as follows:

$$t_{ij} = c_j(t_2) - c_i(t_1) = \frac{||\mathbf{x}_j - \mathbf{x}_i||}{c} + (\theta_j - \theta_i) + u_{ij}, \quad (3)$$

where $u_{ij} \sim \mathcal{N}(0, \sigma_t^2)$. Multiplying both sides of Eq. (3) by c offers:

$$z_{ij} = ||\mathbf{x}_j - \mathbf{x}_i|| + c(\theta_j - \theta_i) + \zeta_{ij}, \quad (4)$$

where $\zeta_{ij} = c \cdot u_{ij}$ is also Gaussian distributed, i.e., $\zeta_{ij} \sim \mathcal{N}(0, \sigma_d^2)$, with $\sigma_d^2 \triangleq c^2\sigma_t^2$. It is noted that ζ_{ij} is assumed independent of $\zeta_{i'j'}$ for any $i' \neq i$ or $j' \neq j$.

III. Cooperative Localization with Approximate Gaussian Belief Propagation (GBP)

Assuming that the time offset θ is estimated, cooperative localization is first addressed (time offset will be studied at Section IV). The range measurements are simplified as follows:

$$z_{ij} = ||\mathbf{x}_j - \mathbf{x}_i|| + \zeta_{ij}. \quad (5)$$

If $\mathbf{X} = \{\mathbf{x}_i \,|\, i \in \mathcal{M}\}$ and $\mathbf{Z} = \{z_{ij} \,|\, (i,j) \in \Xi\}$, then the joint posterior distribution follows from the Bayesian Theorem:

$$\begin{aligned} p(\mathbf{X}|\mathbf{Z}) &\propto p(\mathbf{Z}|\mathbf{X})\, p(\mathbf{X}) \\ &\propto \Big(\prod_{(i,j)\in\Xi} p(z_{ij} \,|\, \mathbf{x}_i, \mathbf{x}_j) \Big) \prod_{i\in\mathcal{M}} p(\mathbf{x}_i), \end{aligned} \quad (6)$$

where the likelihood function $p(z_{ij} \,|\, \mathbf{x}_i, \mathbf{x}_j)$ is given by:

$$\begin{aligned} p(z_{ij} \,|\, \mathbf{x}_i, \mathbf{x}_j) &= \frac{1}{\sqrt{2\pi\sigma_d^2}} \exp\left\{ - \frac{(z_{ij} - ||\mathbf{x}_j - \mathbf{x}_i||)^2}{2\sigma_d^2} \right\} \\ &\propto \exp\left\{ - \frac{z_{ij}^2 - 2z_{ij}\sqrt{(x_j - x_i)^2 + (y_j - y_i)^2}}{2\sigma_d^2} \right. \\ &\qquad \left. - \frac{(x_j - x_i)^2 + (y_j - y_i)^2}{2\sigma_d^2} \right\}, \end{aligned} \quad (7)$$

and the priors $p(\mathbf{x}_i)$ are assumed Gaussian. If $i \in \mathcal{A}$, meaning that there are no location uncertainties, the prior distribution is the Dirac delta function (which can also be considered as Gaussian with variance close to zero). The marginal posterior distribution regarding node i follows:

$$p(\xi_i|\mathbf{Z}) \propto \int p(\mathbf{X}|\mathbf{Z}) \sim \{d\xi_i\}, \quad (8)$$

with $\xi_i \in \{x_i, y_i\}$ and $\sim \{d\xi_i\}$ denoting the integration over all variables collected in $\mathbf{X}$, except for the variable ξ_i. Then, the minimum mean squared error estimator (MMSE) is utilized:

$$\hat{\xi}_i = \int \xi_i\, p(\xi_i|\mathbf{Z})\, d\xi_i. \quad (9)$$

Direct marginalization in Eq. (8) is hard to calculate. Assuming that the x-axis and y-axis coordinates are independent, the posterior distribution is re-written as follows:

$$\begin{aligned} &p\left(\mathbf{x}_i | z_{ij}, \forall j \in \mathcal{N}(i)\right) \\ &\qquad \propto p(x_i)\, p(y_i) \prod_{j\in\mathcal{N}(i)} p(z_{ij} \,|\, x_i, x_j, y_i, y_j). \end{aligned} \quad (10)$$

The joint distribution is factorized and, thus, can be represented by a (bipartite) factor graph, depicted in Fig. 2; the latter shows (for brevity) a single adjacency between nodes i and j.

Sum-Product (or equivalently) Belief Propagation is the message-passing algorithm that will be run on the aforementioned factor graph to obtain the beliefs $b(\xi_i)$; the latter will approximate the marginals $p(\xi_i \,|\, \mathbf{Z})$, $\xi_i \in \{x_i, y_i\}$, $i \in \mathcal{M}$ (with the specific approximations adopted, explained subsequently). Two kinds of messages are exchanged in the factor graph: messages from a factor node to a variable node and messages from a variable node to a factor node. At the l-th iteration, the messages from factor to variable node follow:

$$\begin{aligned} \mu_{f_{ij}\to x_i}^{(l)}(x_i) = \int\int\int f_{ij}\ &\mu_{x_j\to f_{ij}}^{(l-1)}(x_j)\, \mu_{y_i\to f_{ij}}^{(l-1)}(y_i) \\ &\times \mu_{y_j\to f_{ij}}^{(l-1)}(y_j)\, dx_j\, dy_i\, dy_j, \end{aligned} \quad (11)$$

$$\begin{aligned} \mu_{f_{ij}\to y_i}^{(l)}(y_i) = \int\int\int f_{ij}\ &\mu_{y_j\to f_{ij}}^{(l-1)}(y_j)\, \mu_{x_i\to f_{ij}}^{(l-1)}(x_i) \\ &\times \mu_{x_j\to f_{ij}}^{(l-1)}(x_j)\, dy_j\, dx_i\, dx_j, \end{aligned} \quad (12)$$

$$\mu_{f_i\to\xi_i}(\xi_i) = p(\xi_i), \quad (13)$$

with $\xi_i \in \{x_i, y_i\}$, $p(\xi_i)$ the prior distribution of variable ξ_i and $f_{ij} \triangleq f_{ij}(x_i, y_i, x_j, y_j; z_{ij}) \equiv p(z_{ij} \,|\, \mathbf{x}_i, \mathbf{x}_j)$. Notice that the message $\mu_{f_i\to\xi_i}(\xi_i)$ is constant throughout algorithm's execution.

The belief of variable ξ_i is given by:

$$b^{(l)}(\xi_i) \propto \mu_{f_i\to\xi_i}(\xi_i) \prod_{j\in\mathcal{N}(i)} \mu_{f_{ij}\to\xi_i}^{(l-1)}(\xi_i), \quad (14)$$

and finally, the message from variable to factor node is defined as $\mu_{\xi_i\to f_{ij}}^{(l)}(\xi_i) = \mu_{f_i\to\xi_i}(\xi_i) \prod_{j'\in\mathcal{N}(i)/j} \mu_{f_{ij'}\to\xi_i}^{(l-1)}(\xi_i)$,

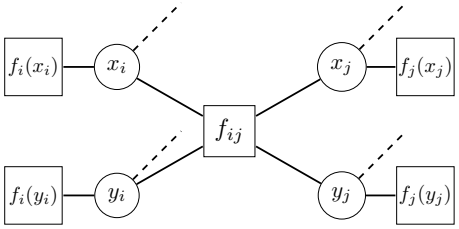

Fig. 2: Factor graph for localization, between node i and node j, with $f_{ij} = p(z_{ij} \,|\, \mathbf{x}_i, \mathbf{x}_j)$ and $f_i(\xi_i)$ the prior of each variable.

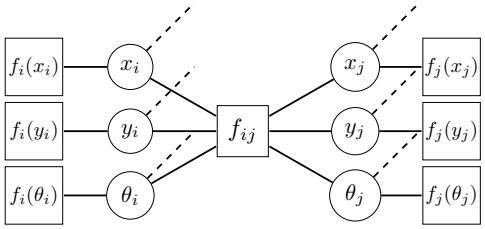

Fig. 3: Factor graph for joint localization and synchronization, between agent node i and anchor node j, with $f_{ij} = p(z_{ij} \,|\, \mathbf{x}_i, \mathbf{x}_j, \theta_i, \theta_j)$ and $f_j(\xi_j) = \delta(\xi_j - m_{\xi_j})$.

$\forall i \in \mathcal{M}$, where notation $\mathcal{N}(i)/j$ means that the set does not include j. Thus, the message can be simplified as follows:

$$\mu^{(l)}_{\xi_i \to f_{ij}}(\xi_i) = \frac{b^{(l)}(\xi_i)}{\mu^{(l)}_{f_{ij} \to \xi_i}}. \tag{15}$$

The computation of the messages in Eqs. (11), (12) in closed-form is intractable due to the square root term in the likelihood function f_{ij}. Work in [9, Eq. (24)], proposed the following linear approximation, based on Taylor expansion around node i's and node j's location estimations $(\hat{x}_i^{(l-1)}, \hat{y}_i^{(l-1)})$ and $(\hat{x}_j^{(l-1)}, \hat{y}_j^{(l-1)})$, in the context of cooperative, joint time offset and location estimation:

$$\begin{aligned}\sqrt{(x_j - x_i)^2 + (y_j - y_i)^2} \simeq \hat{d}_{ij}^{(l-1)} + \lambda_{ij}^{(l-1)}(x_i - \hat{x}_i^{(l-1)}) \\ + \gamma_{ij}^{(l-1)}(y_i - \hat{y}_i^{(l-1)}) + \lambda_{ij}^{(l-1)}(\hat{x}_j^{(l-1)} - x_j) \\ + \gamma_{ij}^{(l-1)}(\hat{y}_j^{(l-1)} - y_j),\end{aligned} \tag{16}$$

with $\hat{d}_{ij}^{(l-1)} = \sqrt{(\hat{x}_j^{(l-1)} - \hat{x}_i^{(l-1)})^2 + (\hat{y}_j^{(l-1)} - \hat{y}_i^{(l-1)})^2}$ the range estimate and

$$\lambda_{ij}^{(l-1)} = \frac{\hat{x}_i^{(l-1)} - \hat{x}_j^{(l-1)}}{\hat{d}_{ij}^{(l-1)}}, \gamma_{ij}^{(l-1)} \quad = \frac{\hat{y}_i^{(l-1)} - \hat{y}_j^{(l-1)}}{\hat{d}_{ij}^{(l-1)}}, \tag{17}$$

the directional derivatives on x-axis and y-axis, respectively. In the proposed cooperative localization algorithm of this section, the time offset is assumed to be estimated using a separate algorithm. It is observed that the RHS of Eq. (16) can be further simplified. Specifically, this work uses the following Taylor-based approximation, which can be shown to be equivalent to the RHS of Eq. (16):

$$\begin{aligned}\sqrt{(x_j - x_i)^2 + (y_j - y_i)^2} \simeq \\ \lambda_{ij}^{(l-1)}(x_i - x_j) + \gamma_{ij}^{(l-1)}(y_i - y_j).\end{aligned} \tag{18}$$

Theorem 1. *For the FG based on Fig. 2 and Eq.* (18)*, under the assumptions of this work, as well as the assumption of Gaussian messages $\mu^{(l-1)}_{\xi_i \to f_{ij}}(\xi_i)$, i.e., $\mu^{(l-1)}_{\xi_i \to f_{ij}}(\xi_i) \sim \mathcal{N}\left(m^{(l-1)}_{\xi_j \to f_{ij}}, (\sigma^{(l-1)}_{\xi_j \to f_{ij}})^2\right)$, the MMSE location estimate of the proposed approximate message passing method, coined as Cooperative Localization with Belief Propagation (CLBP), is given by the mean $m^{(l)}_{\xi_i}$ of the following belief:*

$$b^{(l)}(\xi_i) = \mathcal{N}\Big(m^{(l)}_{\xi_i}, (\sigma^{(l)}_{\xi_i})^2\Big), \tag{19}$$

$$m^{(l)}_{\xi_i} = \left(\sigma^{(l)}_{\xi_i}\right)^2 \left(\frac{m_{f_i \to \xi_i}}{\sigma^2_{f_i \to \xi_i}} + \sum_{j \in \mathcal{N}(i)} \frac{m^{(l)}_{f_{ij} \to \xi_i}}{\left(\sigma^{(l)}_{f_{ij} \to \xi_i}\right)^2} \right), \tag{20}$$

$$\left(\sigma^{(l)}_{\xi_i}\right)^2 = \left(\frac{1}{\sigma^2_{f_i \to \xi_i}} + \sum_{j \in \mathcal{N}(i)} \frac{1}{\left(\sigma^{(l)}_{f_{ij} \to \xi_i}\right)^2} \right)^{-1}. \tag{21}$$

The rest of the parameters needed in the above equations follow:

$$m^{(l)}_{f_{ij} \to x_i} = m^{(l-1)}_{x_j \to f_{ij}} + z_{ij}\, \lambda^{(l-1)}_{ij}, \tag{22}$$

$$\left(\sigma^{(l)}_{f_{ij} \to x_i}\right)^2 = \left(\sigma^{(l-1)}_{x_j \to f_{ij}}\right)^2 + \sigma_d^2, \tag{23}$$

$$m^{(l)}_{f_{ij} \to y_i} = m^{(l-1)}_{y_j \to f_{ij}} + z_{ij}\, \gamma^{(l-1)}_{ij}, \tag{24}$$

$$\left(\sigma^{(l)}_{f_{ij} \to y_i}\right)^2 = \left(\sigma^{(l-1)}_{y_j \to f_{ij}}\right)^2 + \sigma_d^2, \tag{25}$$

$$m^{(l)}_{\xi_i \to f_{ij}} = \frac{m^{(l)}_{\xi_i}\left(\sigma^{(l)}_{f_{ij} \to \xi_i}\right)^2 - m^{(l)}_{f_{ij} \to \xi_i}\left(\sigma^{(l)}_{\xi_i}\right)^2}{\left(\sigma^{(l)}_{f_{ij} \to \xi_i}\right)^2 - \left(\sigma^{(l)}_{\xi_i}\right)^2}, \tag{26}$$

$$\left(\sigma^{(l)}_{\xi_i \to f_{ij}}\right)^2 = \frac{\left(\sigma^{(l)}_{f_{ij} \to \xi_i}\right)^2 \left(\sigma^{(l)}_{\xi_i}\right)^2}{\left(\sigma^{(l)}_{f_{ij} \to \xi_i}\right)^2 - \left(\sigma^{(l)}_{\xi_i}\right)^2}. \tag{27}$$

The proof is omitted due to space constraints and can be found in [13]. To the best of our knowledge, these equations, despite their simplicity, have not appeared in the literature.

1) Differences with prior art: Cooperative Localization with Gaussian Belief Propagation using the Taylor expansion of Eq. (16) has been proposed in [3]; that work exploited a more complex factor graph, utilizing both measurements $z_{i \to j}$ and $z_{j \to i}$ in the form of Eq. (5); thus, the corresponding factor graph required factor f_{ji} as well, and not only f_{ij}. This implies that two-way measurements were needed, in contrast to this work, where only one-way measurements are utilized due to the distance symmetry between two nodes. Furthermore, work in [9] can be modified, so that only localization is performed, while time offset is neglected, i.e., assumed zero; setting in [9, Eqs. (26)-(28) and (31)-(34)] $m^{(l-1)}_{\theta_i \to f_{ij}} = 0$, $m^{(l-1)}_{\theta_j \to f_{ij}} = 0$, $\left(\sigma^{(l-1)}_{\theta_i \to f_{ij}}\right)^2 = 0$, $\left(\sigma^{(l-1)}_{\theta_j \to f_{ij}}\right)^2 = 0$ offers a set of modified equations that coincide with Eqs. (22)-(25) of this work.

IV. Non-cooperative Spatio-temporal Estimation & Localization with Approximate GBP

In this section, the measurement model of Eq. (4) is employed for joint estimation of the clock offset and the location of each agent node, using Belief Propagation through approximate message passing in a non-cooperative environment: the agents receive messages only from anchor nodes. The proposed method is coined as Joint Non-Cooperative Estimation (JNCE). The likelihood function f_{ij} for the joint case follows:

$$f_{ij} = p(z_{ij} \,|\, \mathbf{x}_i, \mathbf{x}_j, \theta_i, \theta_j) \propto \exp\left\{ - \frac{(z_{ij} - ||\mathbf{x}_j - \mathbf{x}_i|| - c\,(\theta_j - \theta_i))^2}{2\sigma_d^2} \right\}, \quad (28)$$

and the joint posterior distribution is given by:

$$p(\mathbf{x}_i, \theta_i | z_{ij}, \forall j \in \mathcal{N}(i)) \propto p(x_i)\, p(y_i)\, p(\theta_i) \prod_{j \in \mathcal{N}(i)} p(z_{ij} \,|\, x_i, x_j, y_i, y_j, \theta_i, \theta_j). \quad (29)$$

The factor graph of the message passing now becomes as in Fig. 3 and the corresponding messages from the factor f_{ij} to ξ_i with $\xi_i \in \{x_i, y_i, \theta_i\}$ are calculated as follows:

$$\mu^{(l)}_{f_{ij}\to\xi_i}(\xi_i) = \int \cdots \int f_{ij} \prod_{\vartheta \in \mathcal{F}_{i,j}/\xi_i} \mu^{(l-1)}_{\vartheta \to f_{ij}}(\vartheta)\, d\vartheta, \quad (30)$$

where $\mathcal{F}_{i,j}$ denotes the set of the variables connected to the factor f_{ij}, i.e., $\mathcal{F}_{i,j} = \{x_i, y_i, \theta_i, x_j, y_j, \theta_j\}$. Since the agents receive messages only from anchors, the messages $\mu^{(l-1)}_{\xi_j \to f_{ij}}$ are equal to a delta distribution $\delta(\xi_j - m_{\xi_j})$, with $\xi_j \in \{x_j, y_j, \theta_j\}$ and m_{ξ_j} the true value of variable ξ_j, for each anchor node j.

TABLE I: Values for messages $\mu^{(l)}_{f_{ij}\to k_i}(k_i), k_i \in \{x_i, y_i\}$

Message	n_1	n_2	n_3	n_4	n_5	n_6
$\mu^{(l)}_{f_{ij}\to x_i}(x_i)$	$\lambda^{(l-1)}_{ij}$	$\sigma^{(l-1)}_{y_i\to f_{ij}}$	m_{x_j}	$m^{(l-1)}_{y_i\to f_{ij}}$	m_{y_j}	$\gamma^{(l-1)}_{ij}$
$\mu^{(l)}_{f_{ij}\to y_i}(y_i)$	$\gamma^{(l-1)}_{ij}$	$\sigma^{(l-1)}_{x_i\to f_{ij}}$	m_{y_j}	$m^{(l-1)}_{x_i\to f_{ij}}$	m_{x_j}	$\lambda^{(l-1)}_{ij}$

The same methodology and approximation of Eq. (18) are employed, as in the cooperative environment, to get the mathematical expressions of the $\mu^{(l)}_{f_{ij}\to\xi_i}$ messages, with $\xi_i \in \{x_i, y_i, \theta_i\}$. The detailed derivation is omitted due to space constraints and can be found in [13]. The resulting messages will be given in the information form:

$$\exp\left\{ - \frac{1}{2}\, J^{(l)}_{f_{ij}\to\xi_i}\, \xi_i^2 + h^{(l)}_{f_{ij}\to\xi_i}\, \xi_i \right\}, \quad (31)$$

with mean value and variance given by:

$$m^{(l)}_{f_{ij}\to\xi_i} = \frac{h^{(l)}_{f_{ij}\to\xi_i}}{J^{(l)}_{f_{ij}\to\xi_i}},\ \left(\sigma^{(l)}_{f_{ij}\to\xi_i}\right)^2 = \frac{1}{J^{(l)}_{f_{ij}\to\xi_i}}. \quad (32)$$

The final equations (in the information form) of the messages $\mu^{(l)}_{f_{ij}\to x_i}$ and $\mu^{(l)}_{f_{ij}\to y_i}$ are proven to be symmetrical and they can be acquired from Eq. (33) according to Table I. The message $\mu^{(l)}_{f_{ij}\to\theta_i}$ is given in Eq. (34). Afterwards, the beliefs and the messages from the variable to the factor node can be calculated with Eqs. (20)-(21) and Eqs. (26)-(27), respectively. To the best of our knowledge, these equations have not appeared in the literature before.

$$\mu^{(l)}_{f_{ij}\to k_i}(k_i) \propto \exp(f(n_1,n_2,n_3,n_4,n_5,n_6,k_i)), f(n_1,n_2,n_3,n_4,n_5,n_6,k_i) =$$
$$\left\{ -\frac{1}{2}\left[\frac{1}{\sigma_d^2} + n_1^2 \left(\frac{1}{\sigma_d^2 + c^2\left(\sigma^{(l-1)}_{\theta_i\to f_{ij}}\right)^2} - \frac{1}{\sigma_d^2} \right) - \left(\lambda^{(l-1)}_{ij}\right)^2 \left(\gamma^{(l-1)}_{ij}\right)^2 \left(\frac{1}{\sigma_d^2 + c^2\left(\sigma^{(l-1)}_{\theta_i\to f_{ij}}\right)^2} - \frac{1}{\sigma_d^2} \right)^2 \left(\frac{\sigma_d^2\, n_2^2}{\sigma_d^2 + n_2^2} \right) \right] k_i^2 \right.$$
$$+ \left[\frac{1}{\sigma_d^2}\,(n_3 + n_1\, z_{ij}) + n_1 \left(\frac{1}{\sigma_d^2 + c^2\left(\sigma^{(l-1)}_{\theta_i\to f_{ij}}\right)^2} - \frac{1}{\sigma_d^2} \right) \left(z_{ij} + m_{x_j}\lambda^{(l-1)}_{ij} + m_{y_j}\gamma^{(l-1)}_{ij} \right) + \frac{c\, n_1\, m^{(l-1)}_{\theta_i\to f_{ij}}}{\sigma_d^2 + c^2\left(\sigma^{(l-1)}_{\theta_i\to f_{ij}}\right)^2} \right.$$
$$\left. \left. - \lambda^{(l-1)}_{ij}\gamma^{(l-1)}_{ij} \left(\frac{1}{\sigma_d^2 + c^2\left(\sigma^{(l-1)}_{\theta_i\to f_{ij}}\right)^2} - \frac{1}{\sigma_d^2} \right) \left(\frac{\sigma_d^2\, n_2^2}{\sigma_d^2 + n_2^2} \right) \left(\frac{n_4}{n_2^2} + \frac{1}{\sigma_d^2}\,(n_5 + n_6\, z_{ij}) \right) \right] k_i \right\}, \quad (33)$$

$$\mu^{(l)}_{f_{ij}\to\theta_i}(\theta_i) \propto \exp(C), C =$$
$$\left\{ -\frac{1}{2} \left[\frac{c^2 \left(\sigma_d^2 + \left(\gamma^{(l-1)}_{ij}\sigma^{(l-1)}_{x_i\to f_{ij}}\right)^2 + \left(\lambda^{(l-1)}_{ij}\sigma^{(l-1)}_{y_i\to f_{ij}}\right)^2 \right)}{\left(\sigma_d^2 + \left(\sigma^{(l-1)}_{x_i\to f_{ij}}\right)^2\right)\left(\sigma_d^2 + \left(\sigma^{(l-1)}_{y_i\to f_{ij}}\right)^2\right)} \right] \theta_i^2 + \left[\frac{c\lambda^{(l-1)}_{ij} m^{(l-1)}_{x_i\to f_{ij}}}{\sigma_d^2 + \left(\sigma^{(l-1)}_{x_i\to f_{ij}}\right)^2} + \frac{c\gamma^{(l-1)}_{ij} m^{(l-1)}_{y_i\to f_{ij}}}{\sigma_d^2 + \left(\sigma^{(l-1)}_{y_i\to f_{ij}}\right)^2} + \frac{c\lambda^{(l-1)}_{ij}\left(\sigma^{(l-1)}_{x_i\to f_{ij}}\right)^2}{\sigma_d^2\left(\sigma_d^2 + \left(\sigma^{(l-1)}_{x_i\to f_{ij}}\right)^2\right)} \right.$$
$$\left. \times \left(m_{x_j} + \lambda^{(l-1)}_{ij} z_{ij} \right) + \frac{c\gamma^{(l-1)}_{ij}\left(\sigma^{(l-1)}_{y_i\to f_{ij}}\right)^2}{\sigma_d^2\left(\sigma_d^2 + \left(\sigma^{(l-1)}_{y_i\to f_{ij}}\right)^2\right)} \left(m_{y_j} + \gamma^{(l-1)}_{ij} z_{ij} \right) - \frac{c}{\sigma_d^2} \left(z_{ij} + m_{x_j}\lambda^{(l-1)}_{ij} + m_{y_j}\gamma^{(l-1)}_{ij} \right) \right] \theta_i \right\}. \quad (34)$$

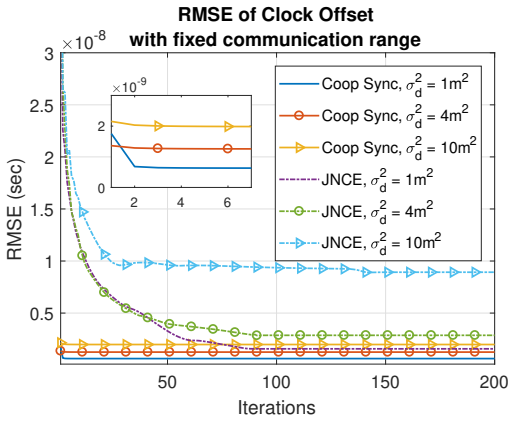

Fig. 4: RMSE of clock offset estimate vs. iterations for different noise power.

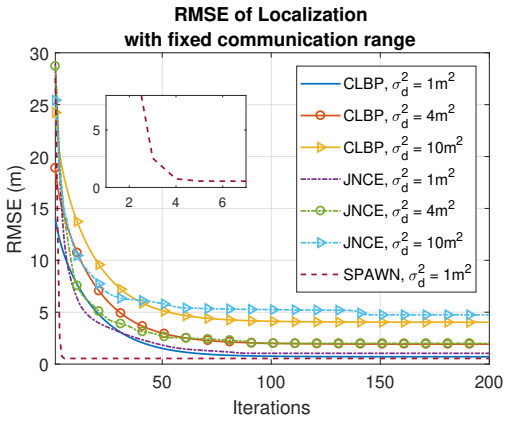

Fig. 5: RMSE of location estimate vs. iterations for different noise power.

V. Numerical Results

A $50 \times 50\,\mathrm{m}^2$ plane is considered with $|\mathcal{M}| = 50$ uniformly distributed agent nodes and $|\mathcal{A}| = 9$ anchor nodes, placed symmetrically at [0 0], [25 0], [50 0], [0 25], [25 25], [50 25], [0 50], [25 50] and [50 50]. The clock offset values are uniformly distributed in $[-8.3 \times 10^{-8}, 8.3 \times 10^{-8}]$ sec. The prior distributions of the agents' positions are considered Gaussian with mean values $m_{x_i} = m_{y_i} = 0$ m and variances $\sigma^2_{x_i} = \sigma^2_{y_i} = 100$ m^2, while the priors of the clock offsets are also Gaussian with $m_{\theta_i} = 0$ sec, $\sigma^2_{\theta_i} = 10^{-15}$ sec^2, $i \in \mathcal{M}$. The maximum communication range is set at 20 m and 35 m for the cooperative and non-cooperative estimation, respectively, unless noted otherwise. It is noted that in the non-cooperative estimation, each agent must communicate with at least four anchor nodes to estimate its clock offset and location unambiguously; that is because the localization problem includes three degrees of freedom: translation, rotation, and reflection, so a connection to an anchor node is needed for each degree of freedom. Since the clock offset θ should also be estimated, a connection to one more anchor node is required. The range measurement noise is assumed to be zero mean Gaussian with variance $\sigma^2_d = 1$ m^2 unless noted otherwise. The maximum number of iterations is set to $N_{iter} = 200$, and all simulation results are averaged from 100 independent Monte Carlo runs. For SPAWN, 4000 particles were used.

The two proposed algorithms, namely CLBP and JNCE, are compared to work in [5] (Coop Sync) for synchronization and in [2] (SPAWN) for localization. For CLBP, the mean values and variances of the messages $\mu^{(0)}_{\xi_i \to f_{ij}}$ are initialized to the prior mean values and variances of each variable ξ_i, with $\xi_i \in \{x_i, y_i\}, i \in \mathcal{M} \cup \mathcal{A}$. For JNCE, the mean values and variances of the same messages are initialized to zeros, with $\xi_i \in \{x_i, y_i, \theta_i\}, i \in \mathcal{M} \cup \mathcal{A}$.

Fig. 4 offers evaluation results for the synchronization problem; it is shown that Coop Sync converges within 4-6 iterations, whereas JNCE needs 100. Moreover, Coop Sync always performs better than JNCE regarding estimation accuracy, as expected, since it estimates only one variable, i.e., the clock offsets of the agents. Namely, Coop Sync achieves a root mean square error (RMSE) of 6×10^{-10} sec under 1 m^2 noise variance and 2×10^{-9} sec under 10 m^2. On the other hand, JNCE performs joint estimation, which means that the synchronization is degraded by the error induced by the location estimates. This difference in the performance of Coop Sync and JNCE is more intense with higher noise variance values. JNCE demonstrates a 1.5×10^{-9} sec RMSE for $\sigma^2_d = 1$ m^2, and for $\sigma^2_d = 10$ m^2, its RMSE error is equal to $\sim 10^{-8}$ sec. However, the messages exchanged in the non-cooperative environment are significantly less due to the lower number of neighbors of each agent; an agent node has $4-7$ neighboring anchors, while in the cooperative case, the number of neighbors is raised to $8-25$ for each agent. Thus, JNCE offers lower communication requirements.

TABLE II: Communication Overhead Comparison

Algorithm	Floating point (fp) numbers/link/iteration	Average iterations	Total load (fp)/link
SPAWN [2]	4000 (particles)	5	20000
CLBP, JNCE	2 (mean & variance)	100	200

Fig. 5 offers localization results and shows that JNCE and CLBP perform very close to SPAWN after convergence. In particular, SPAWN [2] achieves a RMSE of ~ 0.6 m, CLBP approximately 0.8 m and JNCE around 1 m, under a noise variance of 1 m^2. Note that SPAWN converges after 5 iterations, while CLBP and JNCE require ~ 100 iterations. This is due to the Taylor approximation of Eq. (18) that both proposed algorithms exploit to linearize their likelihood function. Regarding higher values of noise, the performance of CLBP and JNCE is expectedly getting worse, but remains similar between the two algorithms. The joint problem, though, is more affected by the synchronization error, and even though CLBP and JNCE behave very close to each other, CLBP outperforms JNCE. The performance of SPAWN is closely related to the particle number; more particles lead to better performance but also higher communication overhead. The

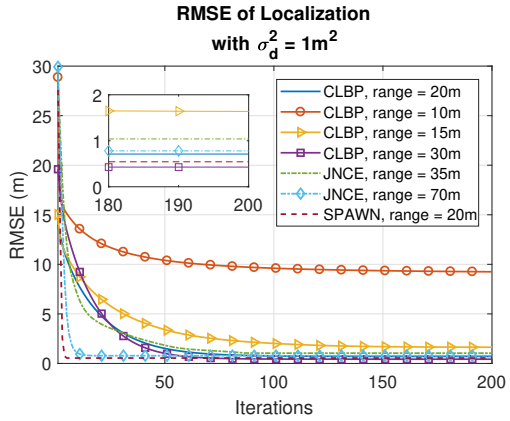

Fig. 6: RMSE of location vs. iterations for different communication ranges.

transmitted messages among neighboring nodes are probability density functions and, thus, need a significant number of particles to be represented. On the contrary, CLBP and JNCE are GBP-based algorithms, so the exchanged messages need only two numbers, i.e., the mean and the variance of each message. According to Table II, SPAWN requires 4000 particles for each transmitted message per iteration and converges after 5 iterations; assuming that each message is represented by floating point (fp) numbers, the total load per communication link amounts to 20000 fp numbers. Although CLBP and JNCE need a larger number of iterations to converge, only 2 fp numbers are exchanged for each message per iteration, leading to a total load of 200 fp numbers per communication link. Therefore, the total communication load per neighboring agent until convergence is 100 times smaller in CLBP and JNCE than in SPAWN. Since SPAWN and CLBP perform cooperative localization, the number of transmitted messages per agent is equal for both algorithms. In non-cooperative localization, JNCE has fewer neighboring nodes per agent, so the communication overhead is more reduced than CLBP.

Fig. 6 demonstrates the performance of the proposed algorithms under fixed noise variance and different values of communication ranges. Under a noise variance of 1 m^2, results for CLBP are expectedly better with 30 m range, compared to 20 m range, even though the difference is small (in the order of 20 cm). This difference increases if the communication range gets reduced by 5 m. The RMSE then becomes 1.8 m, compared to the RMSE of 0.8 m under the 20 m communication range. Especially for the 10 m range, the estimate error is large. The interesting part here is the performance of JNCE when the communication range is increased to 70 m. In this case, JNCE performs slightly better compared to 35 m communication range (with an RMSE drop-off of 20 cm), but much faster; it now needs less than 20 iterations. A range of 70 m in a 50×50 plane means that all agents communicate with all 9 anchors, still resulting in a much lower communication load of JNCE compared to the cooperative environment.

CLBP has been studied further for the extended clock model of Eq. (2), including both time and frequency offset. The latter has been modeled and estimated according to work in [14]. It was found that CLBP performs efficiently, despite the error induced by the frequency and time offset estimation (results were omitted due to space constraints).

VI. Conclusions

This paper proposed two different algorithms: a cooperative approximate GBP for network localization (CLBP) and a joint non-cooperative GBP to simultaneously synchronize and localize the agent nodes of the wireless network (JNCE). Both algorithms are defined by simple algebraic equations, and results showed that for localization, they offer performance close to state-of-the-art but with significantly reduced communication overhead by a factor of 100. Regarding synchronization, state-of-the-art slightly outperforms JNCE for the default setup of the network; however, JNCE has much lower communication overhead due to the requirement for agent communication with anchors only; such number of neighbors per agent is much smaller and can increase the convergence speed of JNCE.

References

[1] N. Patwari, J. Ash, S. Kyperountas, A. Hero, R. Moses, and N. Correal, "Locating the nodes: cooperative localization in wireless sensor networks," *IEEE Signal Processing Mag.*, vol. 22, no. 4, pp. 54–69, 2005.

[2] H. Wymeersch, J. Lien, and M. Z. Win, "Cooperative localization in wireless networks," *Proc. IEEE*, vol. 97, no. 2, pp. 427–450, 2009.

[3] B. Li, N. Wu, H. Wang, and J. Kuang, "Gaussian message passing for cooperative localization in wireless networks," in *IEEE/CIC International Conference on Communications in China (ICCC)*, 2014, pp. 448–452.

[4] A. F. García-Fernández, L. Svensson, and S. Särkkä, "Cooperative localization using posterior linearization belief propagation," *IEEE Trans. Veh. Technol.*, vol. 67, no. 1, pp. 832–836, Jan. 2018.

[5] M. Leng and Y.-C. Wu, "Distributed clock synchronization for wireless sensor networks using belief propagation," *IEEE Trans. Signal Processing*, vol. 59, no. 11, pp. 5404 – 5414, Nov. 2011.

[6] B. Etzlinger, H. Wymeersch, and A. Springer, "Cooperative synchronization in wireless networks," *IEEE Trans. Signal Processing*, vol. 62, no. 11, pp. 2837–2849, 2014.

[7] F. Meyer, B. Etzlinger, F. Hlawatsch, and A. Springer, "A distributed particle-based belief propagation algorithm for cooperative simultaneous localization and synchronization," in *Proc. Asilomar Conf. on Signals, Systems and Computers*, Nov. 2013, pp. 527–531.

[8] B. Etzlinger, F. Meyer, F. Hlawatsch, A. Springer, and H. Wymeersch, "Cooperative simultaneous localization and synchronization in mobile agent networks," *IEEE Trans. Signal Processing*, vol. 65, no. 14, pp. 3587–3602, 2017.

[9] W. Yuan, N. Wu, B. Etzlinger, H. Wang, and J.-M. Kuang, "Cooperative joint localization and clock synchronization based on gaussian message passing in asynchronous wireless networks," *IEEE Trans. Veh. Technol.*, vol. 65, no. 9, pp. 7258–7273, Sep. 2016.

[10] F. Meyer, B. Etzlinger, Z. Liu, F. Hlawatsch, and M. Z. Win, "A scalable algorithm for network localization and synchronization," *IEEE Internet Things J.*, vol. 5, no. 6, pp. 4714–4727, 2018.

[11] W. Yuan, J. Yuan, and D. W. Kwan Ng, "Parametric message-passing for joint localization and synchronization in cooperative networks," in *Proc. IEEE Global Commun. Conf. (Globecom)*, 2020, pp. 1–6.

[12] Q. Yu, Y. Wang, and Y. Shen, "Message-passing-based distributed cooperative simultaneous localization and synchronization in dynamic asynchronous networks," *IEEE Internet of Things Journal*, vol. 11, no. 7, pp. 12 435–12 449, 2024.

[13] M. Samonaki, "Spatio-temporal estimation in wireless networks with message passing," Diploma Thesis, School of ECE, Technical University of Crete, Chania, Greece, Mar. 2022, Supervisor A. Bletsas.

[14] A. Bletsas, "Evaluation of Kalman Filtering for Network Time Keeping," *IEEE Trans. Ultrason., Ferroelect., Freq. Contr.*, vol. 52, no. 9, pp. 1452–1460, Sep. 2005.